Electronic and Optical Properties of Mg2GeO4 Under Pressure Effect: ab Initio Study

Yunxia Zhang (zhangyunxia982@126.com)
JiangXi University of Science and Technology
Li'na Xiao
JiangXi University of Science and Technology

Research Article

Keywords: High pressure, Optical properties, Density functional theory.

Posted Date: July 20th, 2021

DOI: https://doi.org/10.21203/rs.3.rs-627398/v1

Version of Record: A version of this preprint was published at ECS Journal of Solid State Science and Technology on January 20th, 2022. See the published version at https://doi.org/10.1149/2162-8777/ac4d7f.

Electronic and optical properties of Mg_2GeO_4 under pressure effect: ab initio study

Yunxia Zhang[1, a)], Li'na Xiao[1)]

[1]Jiangxi University of Technology, Nanchang 330098, China

Corresponding Author's Electronic mail:

a): zhangyunxia982@126.com

Abstract: We report first-principles studies the structural, elastic, electronic, and optical properties of Mg_2GeO_4 in orthorhombic structure, including pressure dependence of structural parameters, band structures, density of states, and optical constants up to 20 GPa. The calculated structural parameters are in good agreement with the available experimental values at zero pressure. The mechanical stability of Mg_2GeO_4 has been confirmed by calculation of the elastic constants. And the non-uniform pressure dependence of the lattice parameters may also mean that Mg_2GeO_4 undergoes anisotropic compression. Meanwhile, the pressure dependence of the electronic band structure, density of states and partial density of states of Mg_2GeO_4 up to 20 GPa were presented. The band structures show a direct band gap for this compound and the calculated band gaps expend with increasing pressure. Moreover, the evolution of the dielectric function, absorption coefficient ($\alpha(\omega)$), reflectivity ($R(\omega)$), and the real part of the refractive index ($n(\omega)$) at high

pressure are also presented. According to our work, we found that the optical properties of Mg_2GeO_4 undergo a blue shift with increasing pressure.

Keywords: High pressure; Optical properties; Density functional theory.

1. Introduction

In recent years, the germanate forsterite compounds has attracted tremendous attention to be functional materials owing to their potential technological applications and various unique properties, such as optical catalytic activities, unusual magnetic, and ferroelectric properties[1-4]. Among these compounds, Mg_2GeO_4 is an end-member of the olivine solid solution series and they are regarded as the most important components in the Earth's upper mantle[5]. An understanding of electronic and optical properties in these systems is also fundamental interest in solid-earth geochemistry and geophysics[6-7].

At room temperature and normal pressure, the Mg_2GeO_4 has an orthorhombic crystal structure with the space group *Pnma*, in which four formula units are contained in the unit cell[8]. In the crystal, Ge atoms are coordinated with four O atoms to form GeO_4 tetrahedra, as in other silicate minerals. The GeO_4 tetrahedra are linked together by the Mg atoms lying between them[9]. Due to its unusual characteristics, many researchers have investigated the structural, mechanical and electronic

properties of Mg_2GeO_4 at ambient pressure. B. Reynard *et al* used Raman spectroscopic diffraction to determine that Mg_2GeO_4 crystals structural at low pressures[10]. To explore the feasibility of this mechanism, A. Schubnel *et al* performed deformation experiments on germanate forsterite compounds under differential stress at high pressure[11]. These studies have demonstrated that Mg_2GeO_4 structure can metastably exist up to 20 GPa at ambient temperature. Moreover, it is well known that the optical properties of materials rely heavily on their electronic structures. High pressure is an effective approach which can be used to regulate and control the requisite electronic structure and optical properties of these oxide-based materials. Here, we provide a clear picture about pressure dependence of Mg_2GeO_4 geometrical structure, electronic band structure and optical properties up to 20 GPa. In this paper, the evolution of the dielectric function, absorption coefficient ($\alpha(\omega)$), reflectivity ($R(\omega)$), and the real part of the refractive index ($n(\omega)$) at high pressure are also presented. The aim of the present study is to investigate the Mg_2GeO_4 properties of interest in the orthorhombic structure, with emphasis on their dependence on hydrostatic pressure.

2. Method of calculation

The present calculations were performed with the Vienna *ab* initio Simulation Package code (VASP), which makes use of the Perdew-Burke-Ernzerhof (PBE) exchange-correlation function applying

the projector augmented wave method with GGA-PBE potentials[12-14]. The wave functions were expended in-plane waves up to the kinetic energy cutoff of 750 eV and convergence criteria for energy of 10^{-4} eV are selected. A 4×2×7 Brillouin-Zone (BZ) k-point sampling is used in the calculation. The band structure calculations have been carried out following a path along the most high symmetry points G, Z, T, Y, S, X, U, and R. The internal coordinates of these points are (0, 0, 0), (0, 0, 0.5), (-0.5, 0. 0.5), (-0.5, 0, 0), (-0.5, 0.5, 0), (0, 0.5, 0), (0, 0.5, 0.5), and (-0.5, 0.5, 0.5) in the first Brillouin zone, respectively. We adopt the experimental lattice parameters of Mg_2GeO_4 with *a*=10.304 Å, *b*=6.032 Å, and *c*= 4.913 Å, to build the initial crystal structure[8]. During the geometry optimization, the space group of the Mg_2GeO_4 crystal has been constrained to *Pnma*. Thus, no structural phase transition will be considered in this study.

Moreover, the different band and electronic density to states can induce different dielectric response. The dielectric function $\varepsilon(\omega) = \varepsilon_1(\omega) + i\varepsilon_2(\omega)$ is an important function to describe the optical properties. Because the imaginary part $\varepsilon_2(\omega)$ is the pandect of optical properties, we use formula (1) to calculate the $\varepsilon_2(\omega)$ of Mg_2GeO_4. In the formula, the superscript c and ν represent conduction and valence bands, respectively. $\hat{u}$ is the electric-field vectors of incident light field.

$$\varepsilon_2(\omega) = \frac{2e^2\pi}{\Omega\varepsilon_0}\sum_{k,v,c}|\langle\psi_k^c|\hat{u}\times r|\psi_k^v\rangle|^2\,\delta(E_k^c - E_k^v - E) \qquad (1)$$

The real part $\varepsilon_1(\omega)$ was calculated by the Kramers-Kronig relation (formula (2)). In the relation, p repents the principal value of the integral. The formula (1) and (2) show the $\varepsilon_1(\omega)$ and $\varepsilon_2(\omega)$ are the response of the incident light.

$$\varepsilon_1(\omega) = 1 + \frac{2}{\pi} p \int_0^{\infty} \frac{\omega' \varepsilon_2(\omega')}{\omega'^2 - \omega^2} d\omega' \qquad (2)$$

And optical constants are important in designing optical devices. We use the following three formulas (3)-(5) to calculate the optical constants: the absorption coefficient ($\alpha(\omega)$), reflectivity ($R(\omega)$), and the real part of the refractive index ($n(\omega)$)[15-16].

$$\alpha(\omega) = \sqrt{2}[\sqrt{\varepsilon_1{}^2 + \varepsilon_2{}^2} - \varepsilon_1(\omega)]^{1/2} \qquad (3)$$

$$R(\omega) = \left|\frac{\sqrt{\varepsilon_1(\omega)+j\varepsilon_2(\omega)}-1}{\sqrt{\varepsilon_1(\omega)+j\varepsilon_2(\omega)}+1}\right|^2 \qquad (4)$$

$$n(\omega) = [\sqrt{\varepsilon_1{}^2(\omega) + \varepsilon_2{}^2(\omega)} + \varepsilon_1(\omega)]^{1/2}/\sqrt{2} \qquad (5)$$

3. Results and discussions

3.1 Structural properties

We first performed an optimization of the geometry of the lattice parameters within both the GGA and LDA schemes. The optimized results of the primitive cell of Mg_2GeO_4 in orthorhombic structure are shown in Table I. Together with the available experimental data and various theoretical methods results for comparison. The lattice parameters were computed at zero temperature. Thus, the lattice parameters should have smaller values than the experimental ones obtained at the room temperature. A detailed comparison between calculation and experiment

implies that the LDA method yields better lattice constants values for this type of germanate systems than the GGA method. Therefore, we calculated the self-consistent electronic structure at optimal lattice constants and internal structural parameters form the LDA calculation in present work below.

As expected, the structural parameters *a, b,* and *c* decrease with increasing pressure. Pressure dependence of the lattice parameters *a*, *b*, and *c* of Mg_2GeO_4 are shown in Fig. 1. When applying a linear fitting in the whole pressure range, the linear compressibility of the lattice parameters *a*, *b,* and c is 0.006 GPa^{-1}, 0.025 GPa^{-1}, and 0.012 GPa^{-1} up to 20 GPa, respectively. These calculated results indicate that the linear compressibility along *b* axis is significantly higher than *a* and *c* axes, which shows that the intermolecular bonding along the *b* axis is softer and hence easily compressible than other crystallographic axes. The non-uniform pressure dependence of the lattice parameters may also mean that Mg_2GeO_4 undergoes anisotropic compression. Moreover, by increasing pressure, the unit cell volumes are readily compressed. The variation of the unit cell volume for Mg_2GeO_4 with pressure is shown in Fig. 2. The red line is the fitting results by using the third-order Birch-Murnaghan equation of state[17], $P = \frac{3}{2}B_0[\left(\frac{V}{V_0}\right)^{-7/3} - (\frac{V}{V_0})^{-5/3}] \times \left\{1 + \frac{3}{4}(B_0' - 4)\,[\left(\frac{V}{V_0}\right)^{-2/3} - 1]\right\}$, where B_0 is the bulk modulus, B_0' is the derivative of bulk modulus at ambient pressure, and V_0 the volume at

ambient pressure. At 20 GPa the volume compression is V/V_0=86.87%, (V=281.11 Å^3, V_0=323.59 Å^3). The bulk modulus at ambient pressure and temperature is B_0 =104.5 GPa and its derivative is $B'_0 = 9.72$. The high bulk modulus shows that the sample is hardly to be compressed under pressure.

In order to study the mechanical stability of Mg_2GeO_4, we calculated the second-order elastic constants C_{ij} using the "stress-strain method". The nine independent elastic constants of orthorhombic Mg_2GeO_4 at 0 GPa are shown in Table II. For orthorhombic crystal, the mechanical stability requires the elastic constants satisfying the well-known Born stability criteria[18]: $C_{11}+C_{22}-2C_{12}>0$; $C_{11}+C_{33}-2C_{13}>0$; $C_{33}+C_{22}-2C_{23}>0$ and $(C_{11} + C_{22} + C_{33} + 2C_{12} + 2C_{13} + 2C_{21}) > 0$ and $C_{ii}>0$. It is found that our calculated elastic constants can meet the mechanical stability conditions mentioned above. And in Fig. 3, we show the pressure dependence of elastic constants of the orthorhombic Mg_2GeO_4 at 0 K, to the best of our knowledge, no experimental and theoretical are available. It can be seen that the elastic constant C_{13}, C_{12}, C_{22}, C_{23}, C_{11}, and C_{33} increase monotonically with the increasing pressure. The elastic constant C_{66} increase firstly and then decrease as pressure increases. However, the elastic constants C_{44} and C_{55} have little change with the increasing pressure.

Furthermore, according to the study of sin'ko et al. the elastic

constants of a crystal under pressure are known as: $C'_{\alpha\alpha} = C_{\alpha\alpha} - P$, $C'_{\alpha\beta} = C_{\alpha\beta} + P$ $(\alpha = 1, 2, \ldots, 6;\ \beta = 1, 2, \ldots, 6)$. Hence, for orthorhombic crystals under pressure, the mechanical stability requires that the elastic constants satisfy the following stability criteria: $C_{ii} - P > 0$, $(C_{11} + C_{22} + C_{33} + 2C_{12} + 2C_{13} + 2C_{23} + 3P) > 0$, and

$$C_{11} + C_{22} - 2C_{12} - 4P > 0 \quad (7)$$

$$C_{11} + C_{33} - 2C_{13} - 4P > 0 \quad (8)$$

$$C_{22} + C_{33} - 2C_{23} - 4P > 0 \quad (9)$$

Fig. 4 shows the mechanical stabilities of orthorhombic Mg_2GeO_4 as a function of pressure. Clearly, the values of $C_{11} + C_{22} - 2C_{12} - 4P$ decreases rapidly with the increase of pressures, while the value of $C_{22} + C_{33} - 2C_{23} - 4$ and $C_{11} + C_{33} - 2C_{13} - 4$ decreases comparatively slowly. And the calculated results for all satisfy the above stability criteria over the hole pressure range investigated, implying that the structure is mechanically stable within 20 GPa.

3.3 Band structures and density of states

At room temperature and normal pressure, Mg_2GeO_4 is an insulator. The effect of pressure on the electronic structure of Mg_2GeO_4 is an important parameter for better understanding its optical properties[19-20]. For this reason, the aim of this part of the work is to understand the electronic band structures, density of states (DOS) and partial density of states (PDOS) of Mg_2GeO_4 with pressure from 0 to 20 GPa.

The band structure of Mg_2GeO_4 at ambient pressure, 5 GPa, 10 GPa, and 20 GPa presented in Fig. 5. Bothe the valence band maximum (VBM) and the conduction band minimum (CBM) are located at the high symmetry G point. It means that Mg_2GeO_4 is a direct band gap material. At ambient pressure, the band gap for Mg_2GeO_4 is 3.92 eV at the LDA level. However, as the pressure increases, the conduction and valence band shift to higher and lower energies, respectively. The shifts of the conduction and valence band result in an increasing band gap. The calculated band gaps of Mg_2GeO_4 as functions of pressure are shown in Fig. 6. For example, the band gap of Mg_2GeO_4 shifts from 4.09 eV under a pressure of 5 GPa to 4.26 eV under a pressure of 10 GPa and then to 4.51 eV under a pressure of 20 GPa. One can see that the band gap increases smoothly under compression without any significant discontinuity. But in different pressure ranges, the average increase of band gap is different. When applying a linear fit in the lower and higher pressure range, respectively, the average increase of the band gap up to 5 GPa is 0.036 eV/GPa and 0.031 eV/GPa from 5 to 10 GPa and 0.025 eV/GPa from 10 to 20 GPa. That is to say, the band gap as well as the optical response might be tunable by exerting a pressure on Mg_2GeO_4. Moreover, the pressure response of the band gap and electrical conductivity is vitally significant for practical applications and may guide in photoelectric device design[21].

To study the pressure effect on electronic properties, the results of the density of states (DOS) and the partial density of states (PDOS) of Mg_2SiO_4 are shown in Fig. 7. According to the PDOS, The conduction band energy between 3.32 and 5.76 eV mainly comes from Ge 4s and O 2p, while the conduction band energy between 6.44 and 8.91 eV mainly comes from Ge 4p and a strong hybridization can found between Mg 2p, Ge 4s, and O 2p states. But the valence band energy near the Fermi level between -5.29 and -0.63 eV mainly comes from O 2p. The band energy between -19.23 and -16.12 eV mainly comes from O 2s, while O 2p contributes little in this energy range. When increasing pressure, a slight shift of the peaks of DOS for conduction and valence bands are shifted to higher and lower range. For example, the main peak of O 2p orbital in the valence band energy of Mg_2GeO_4 shifts from -1.01 eV under a pressure of 5 GPa to -1.18 eV under a pressure of 10 GPa and then to -1.24 eV under a pressure of 20 GPa. The bottom of the conduction band shifts from 3.04 eV under a pressure of 5 GPa to 3.35 eV under a pressure of 10 GPa and then to 3.78 eV under a pressure of 20 GPa. As a result, the shifts of the conduction and valence band are consistent with the band structures. This energy shift results in the enlargement of band gap substantially, which are in agreement with band structures and explain the band structures as well[22].

3.3 Optical properties

We are interested in the effect of pressure on the optical properties. Figure 8 shows the reflectivity ($R(\omega)$), absorption coefficient ($\alpha(\omega)$), refractive index ($n(\omega)$) and the extinction coefficient ($k(\omega)$) at 0, 10, and 20 GPa with photon energy ranging from 0 to 30 eV. From Fig. 8, we can see that peaks of optical constants shift to higher energies with increasing pressure, which meaning undergo a blue shift. As shown in Fig. 8 (a), the values of $R(\omega)$ of a main peak are at 10.74 eV under normal pressure and the reflectivity further decrease rapidly in the high energy region. With increase pressures, the main peak of $R(\omega)$ shifts to a higher energy region from 11.06 eV under a pressure of 10 GPa to 11.26 eV under a pressure of 20 GPa. Notably, as can be seen in Fig. 6 (b), at ambient pressure, the strongest absorptive behavior around the 10.11 eV. Additionally, the optical band gap of Mg_2GeO_4 can be determined by the following relation: $(\alpha h\nu)^2 = A(h\nu - E_g)$, where A is a constant and E_g is the optical band gap, h is Planck's constant, and ν is the frequency of the incident photon[23]. The optical band gap was increase from 3.92 to 4.51 eV as the pressure increase from 0 to 20 GPa, which is consistent with the calculated band structures.

The optical properties of materials can be described by the refractive index and the extinction coefficient, and are closely related to dielectric constant. The refractive index and the extinction coefficient have also been calculated for Mg_2GeO_4 under 0, 10, and 20 GPa as displayed in

Figs. 8 (c) and 8 (d), respectively. The $k(\omega)$ shows a main peak at around 9.61 eV and 10.43 eV for Mg_2GeO_4 at 0 and 20 GPa, respectively. The $n(\omega)$ shows a main peak at around 3.97 eV and 4.51 eV for Mg_2GeO_4 at 0 and 20 GPa, respectively. Both the refractive index and the extinction coefficient shift toward the higher-energy region when the pressure increases, which is consistent with absorption coefficient ($\alpha(\omega)$) and reflectivity ($R(\omega)$).

Meanwhile, the dielectric function is a crucial physical parameter describing the optical properties, and it reflects the linear response of materials to electromagnetic radiation. As shown in Fig. 9 (b), we notice there is a main peak at 9.09 eV in the $\varepsilon_2(\omega)$ spectrum of Mg_2GeO_4 under no-pressure conditions. This peak takes its origin from the optical transitions between Ge 4p states in the conduction band. When the pressure increases from 0 to 20 GPa, the spectrum exhibits a significant blue shift without any notable shape changes. From Fig. 9 (a), the peaks of $\varepsilon_1(\omega)$ follow a similar trend of $\varepsilon_2(\omega)$ when applying an increasing pressure on Mg_2GeO_4. The zero frequency dialectric constant $\varepsilon_1(0)$ are found to be about 2.04, 2.01, and 1.98 at 0, 10, and 20 GPa, respectively. Interestingly, it also can be seen from Fig. 9 (b), as the pressure is increased to 20 GPa, the maximum peak of $\varepsilon_2(\omega)$ has moved from 9.09 to 9.92 eV. According to the non-uniform pressure dependence of the structural properties, both the energy gap growth and the blue shift of the

optical properties are more strongly pronounced in the low pressure range compared to the high pressure region. We believe that the above results can help to offer a theoretical basis for the experiments and applications of alkaline-earth aluminates crystals.

4. Conclusion

Structural parameters, electronic and optical properties of Mg_2GeO_4 have been investigated using the plane-wave ultrasoft pseudo-potential technique based on the first principles density functional theory. The non-uniform pressure dependence of the lattice parameters may also mean that the Mg_2GeO_4 undergoes anisotropic compression. And The bulk modulus at ambient pressure and temperature is B_0 =104.5 GPa and its derivative is $B'_0 = 9.72$. Meanwhile, the pressure dependence of the electronic band structure, density of states and partial density of states of Mg_2GeO_4 were presented. It is shown that Mg_2GeO_4 is an insulator with a direct gap of 3.92 eV, and a pressure induced increase of the band gap is observed. Moreover, the complex dielectric function, absorption coefficient, reflectivity, refractive index, and extinction coefficient are calculated and analyzed. According to our work, we found that the optical properties of Mg_2GeO_4 undergo a blue shift with increasing pressure.

ACKNOWLEDGMENTS

Parts of the calculations were performed at the Center for Computational Science of CASHIPS, the ScGrid of Supercomputing

Center, and the Computer Network Information Center of the Chinese Academy of Sciences.

References

[1]Aguado. A, Madden P. A, Phys. Rev. Lett. **94** (2005) 68501.

[2]G. Bulman, P. Barletta, J. Lewis, N. Baldasaro, M. Manno, A. B. Cohen, B. Yang, Nat. Commun. **7** (2016) 10302.

[3]X. Fan, G. Zeng, C. LaBounty, J. E. Bowers, E. Croke, C. C. Ahn, A. Majumdar, A. Shakouri, Appl. Phys. Lett. **78** (2001) 1580.

[4]Y. Du, J. Xu, B. Paul, P. Eklund, Appl. Mater. Today. **12** (2018) 366.

[5]S. Ghahari, E. Ghafari, N. Lu, Constr. Build. Mater. **146** (2017) 755.

[6]E. N. Hurwitz, M. Asghar, A. Melton, B. Kucukgok, L. Su, M. Orocz, M. Jamil, N. Lu, I. T. Ferguson, J. Electron. Mater. **40** (2011) 513.

[7]N. Lu, I. Ferguson, Semi. Sci. Tech. **28** (2013) 074023.

[8]B. V. Dreele, A. Navrotsky, Acta. Cryst. **B33** (1977) 2287.

[9]Dharmendra Y, Upendra K, Shail U, J. Adv. Ceramics. **8(3)** (2019) 377.

[10]B. Reynard, P. E. Petit, F. Guyot, P. Gillet, Phys. Chem. Minerals. **20** (1994) 556.

[11]A. Schubnelm, F. Brunet, N. Hilairet, J. Gasc, Y. B. Wang, H. W. Green, Science. **341** (2013) 1377.

[12]P. E. Blochl, Phys. Rev. B. **50** (1994) 17953.

[13]Perdew J. P, Zunger A, Phys. Rev. B 23 (1981) 5048.

[14]Ceperley D. M, Alder B. J, Phys. Rev. Lett. 45 (1980) 566.

[15]Matsumoto Y, J. Solid State Chem. 126, 227 (1996).

[16]Devanathan R, Yu N, Sickafus K. E, Nastasi M, J. Nucl. Mater. 232 (1996) 59.

[17]F. Birch, J. Geophys. Res.91, 4949 (1986).

[18]Wu Z. J, Hao X. F, Liu X. J, Meng J, Phys. Rev. B 75 (2007) 054115.

[19]Devanathan R, Yu N, Sickafus K. E, Nastasi M, J. Nucl. Mater. 232 (1996) 59.

[20]Isobe T, Daimon K, Matsubara T, Hikichi Y, Ceram. Int. 33 (2007) 1211.

[21]Saha S, Sinha T. P, and Mookerjee A, Phys. Rev. B 62, (2000) 8828.

[22]Grzyb T, Szczeszak A, Rozowska J, J. Phys. Chem. C, 116 (2012) 3219.

[23]F. Urbach, Phys. Rev. 92, (1953) 1324.

Table caption

Table. I. The lattice parameters and volume of Mg_2GeO_4 using both LDA and GGA functional along with the previous experimental values[7].

Parameters	*a (Å)*	*b (Å)*	*c (Å)*	*V(Å^3)*
GGA	10.534	6.156	4.991	323.59
LDA	10.234	5.998	4.867	298.73
Expt.	10.304	6.032	4.913	305.36

Table II. The calculated nine independent elastic constants (GPa) for orthorhombic Mg_2GeO_4 at 0 GPa using LDA functional.

	C_{11}	C_{22}	C_{33}	C_{44}	C_{55}	C_{66}	C_{12}	C_{13}	C_{23}
This work	165.91	191.86	273.58	57.17	62.79	38.13	58.43	56.65	57.07

Figure Captions

Fig. 1. The lattice parameters of Mg_2GeO_4 under high pressure up to 20 GPa.

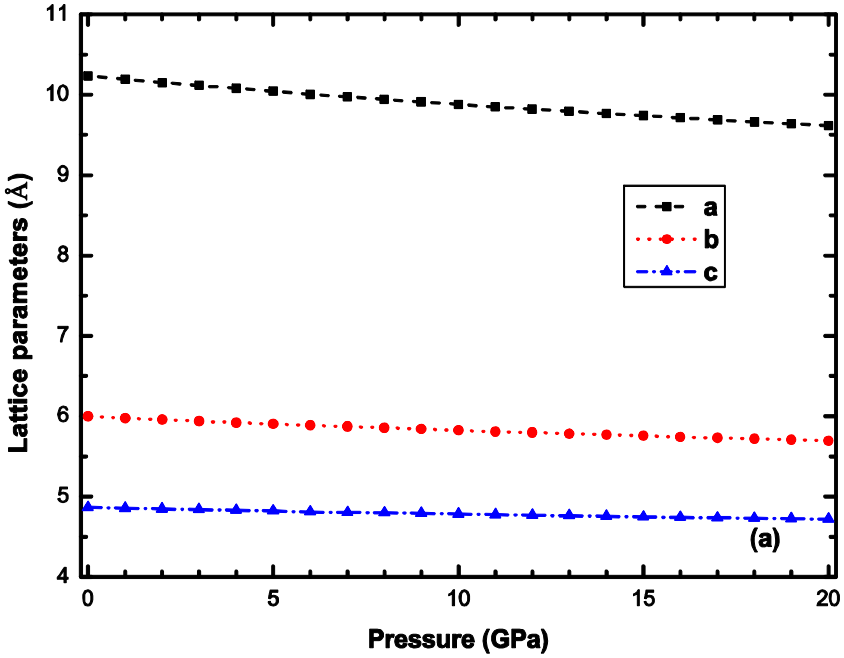

Fig. 2. The unit cell volume compressibility of Mg_2GeO_4 at zero temperature.

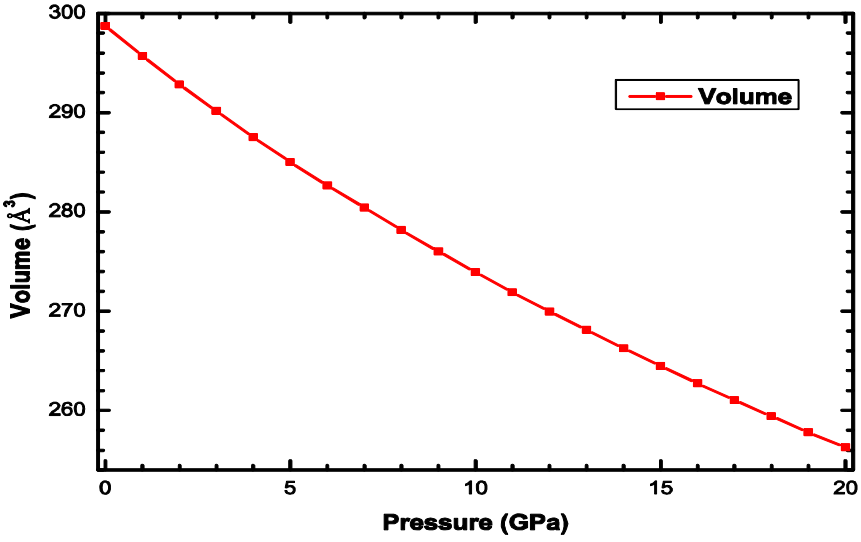

Fig. 3. Calculated elastic constants of orthorhombic Mg_2GeO_4 as a function of pressure.

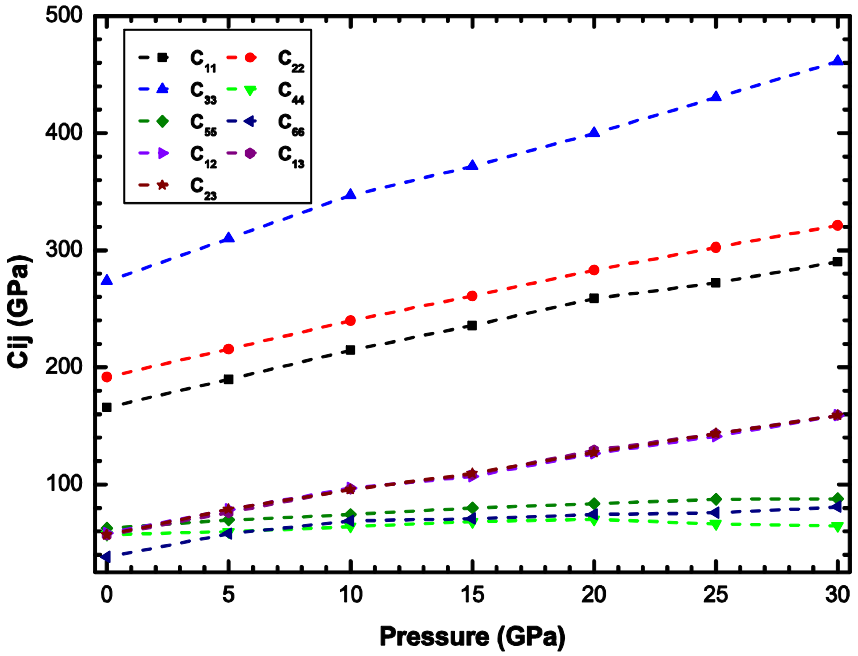

Fig. 4. Mechanical stabilities of orthorhombic Mg_2GeO_4 as a function of pressure.

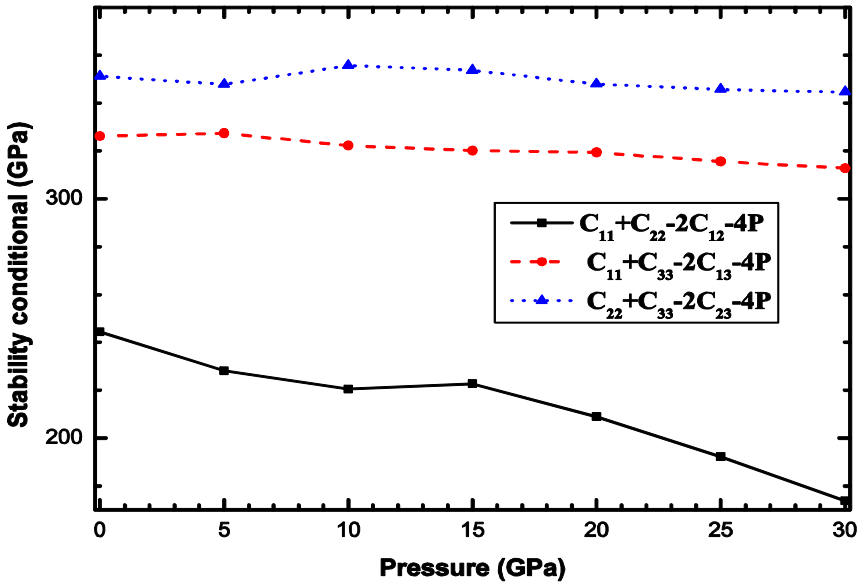

Fig. 5. The band structures of Mg_2GeO_4 at 0 GPa, 5 GPa, 10 GPa, and 20 GPa, respectively. The red dashed line is marked the Fermi level.

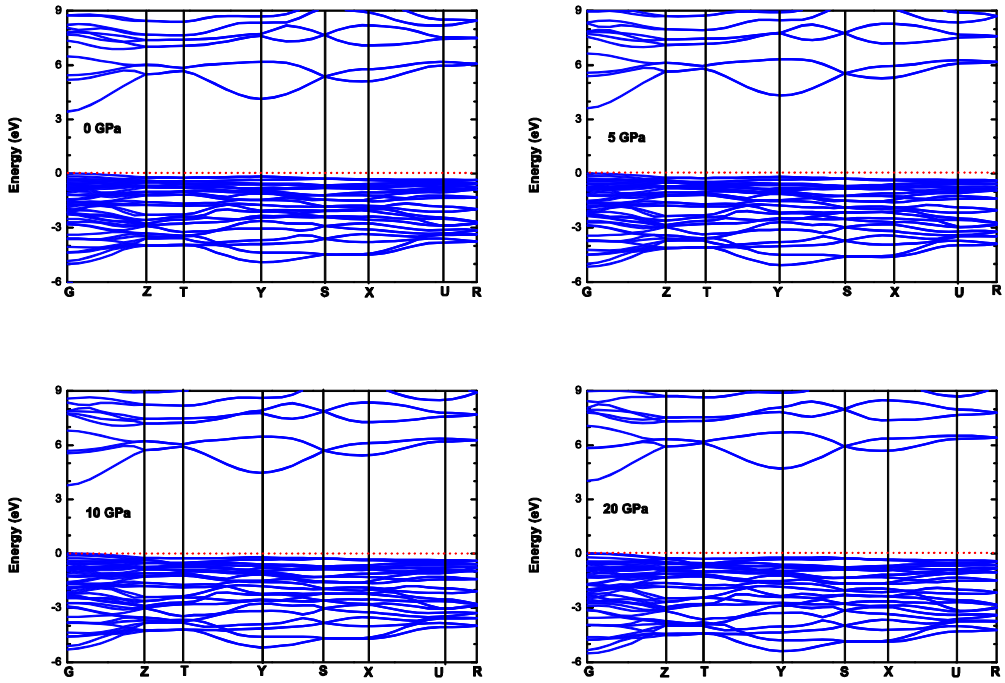

Fig. 6. The dependence of the band gap of Mg_2GeO_4 on pressure.

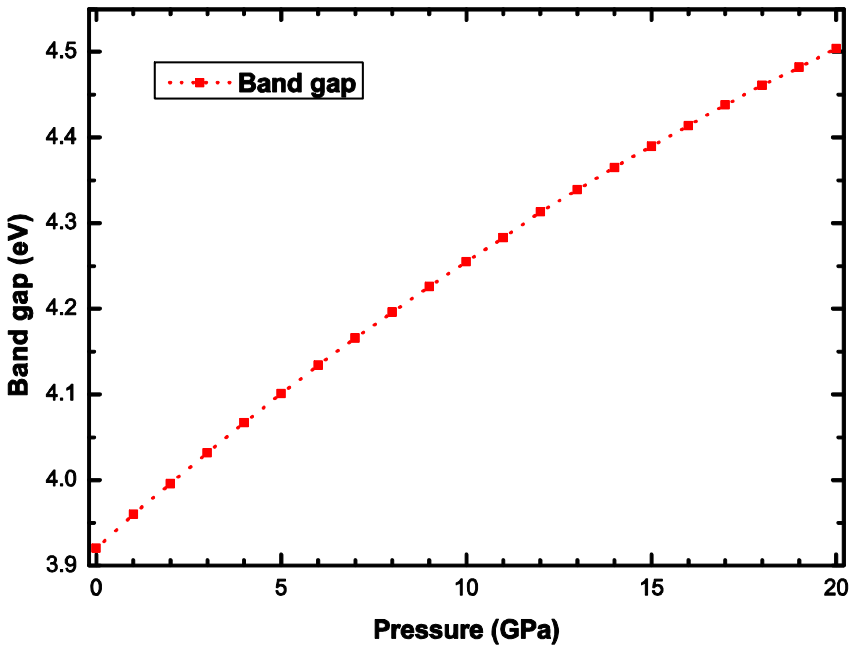

Fig. 7. The density of state (PDOS) and partial density of state (PDOS) of Mg_2GeO_4 at 0 GPa, 5 GPa, 10 GPa, and 20 GPa, respectively. The red dashed line is marked the Fermi level.

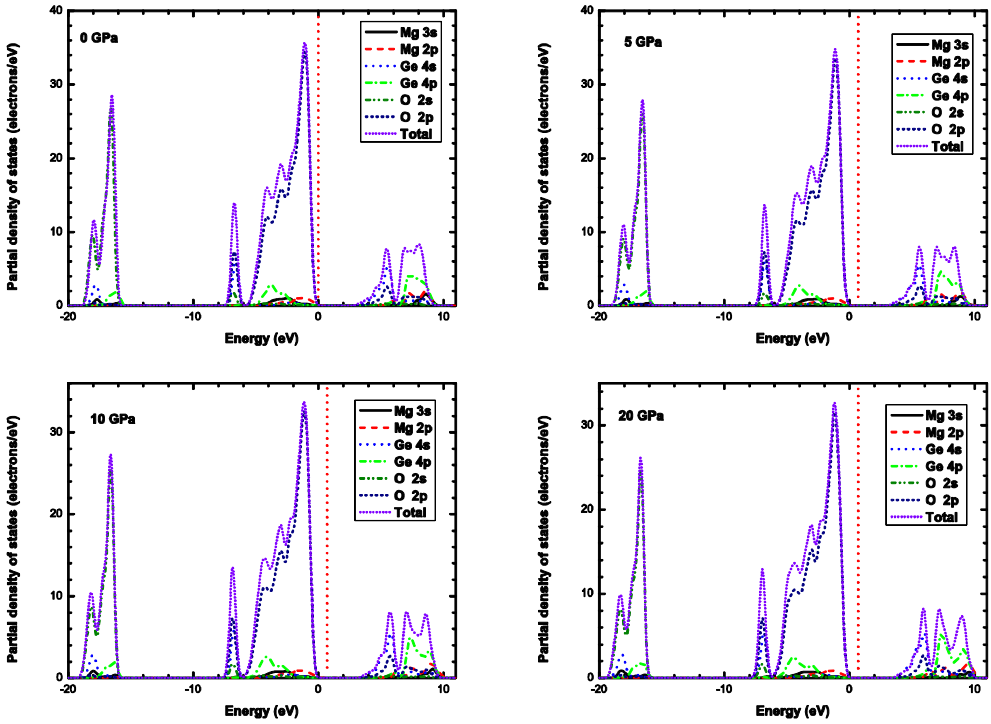

Fig. 8. The optical constants of Mg_2GeO_4: (a) reflectivity (R(ω)); (b) absorption coefficient (α(ω)); (c) the refractive index (n(ω)); and (d) the extinction coefficient (k(ω)).

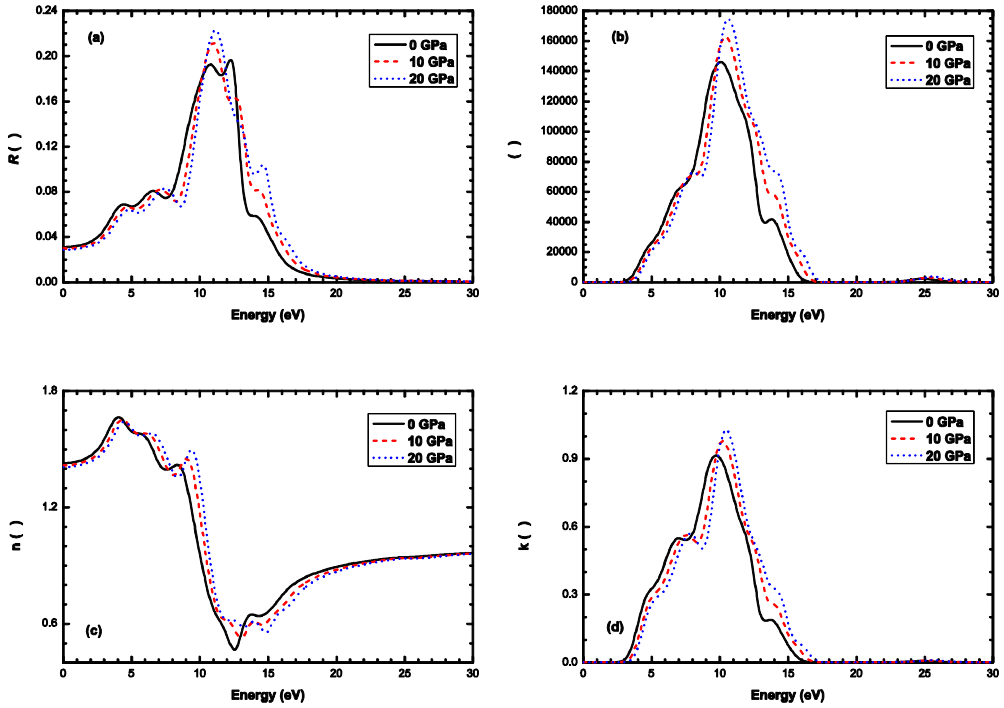

Fig. 9. The dependence of the complex dielectric function of Mg_2GeO_4 at 0 GPa, 10 GPa, and 20 GPa, respectively. (a) the imaginary part $\varepsilon_2(\omega)$ and (b) the real part $\varepsilon_1(\omega)$.